Development 119, 1079-1091 (1993)
Printed in Great Britain © The Company of Biologists Limited 1993

Defects in mesoderm, neural tube and vascular development in mouse embryos lacking fibronectin

Elizabeth L. George*, Elisabeth N. Georges-Labouesse†, Ramila S. Patel-King, Helen Rayburn and Richard O. Hynes‡

Howard Hughes Medical Institute, Center for Cancer Research, and Department of Biology, Massachusetts Institute of Technology, Cambridge, Massachusetts 02139, USA

*Present address: Vascular Research Division, Department of Pathology, Brigham and Women's Hospital, Harvard Medical School, Boston, Massachusetts 02115, USA
†Present address: LGME-CNRS, Inserm U 184, Strasbourg 67085, France
‡Author for correspondence

SUMMARY

To examine the role of fibronectin in vivo, we have generated mice in which the fibronectin gene is inactivated. Heterozygotes have one half normal levels of plasma fibronectin, yet appear normal. When homozygous, the mutant allele causes early embryonic lethality, proving that fibronectin is required for embryogenesis. However, homozygous mutant embryos implant and initiate gastrulation normally including extensive mesodermal movement. Neural folds also form but the mutant embryos subsequently display shortened anterior-posterior axes, deformed neural tubes and severe defects in mesodermally derived tissues. Notochord and somites are absent; the heart and embryonic vessels are variable and deformed, and the yolk sac, extraembryonic vasculature and amnion are also defective. These abnormalities can be interpreted as arising from fundamental deficits in mesodermal migration, adhesion, proliferation or differentiation as a result of the absence of fibronectin. The nature of these embryonic defects leads to reevaluation of suggested roles for fibronectin during early development based on results obtained in vitro and in embryos of other species.

Key words: fibronectin, mesoderm, vasculogenesis, gastrulation, mouse

INTRODUCTION

Fibronectins (FNs) are a group of closely related glycoproteins encoded by a single gene, whose transcript is alternatively spliced at three positions. FNs are major constituents of the extracellular matrix and promote cell adhesion and spreading, cell migration and cytoskeletal organization (reviewed in Hynes, 1990). The extensive structure-function analyses of FNs and their effects on cells in vitro clearly indicate important functions for these proteins in affecting cell behavior. Since expression of FN is widespread in embryos and in adult tissues and is altered in physiological and pathological processes including cancer, hemostasis and thrombosis, fibrosis and wound healing, it is widely believed that FNs play important roles in development and in adult physiology. In particular, FNs have been shown to promote the migration of many cells in vitro and are present in most areas of active cell migration in embryos. Furthermore, synthesis of FN is stimulated during wound healing, which typically involves migration on a FN-fibrin matrix (Clark, 1988; ffrench-Constant et al., 1989; Hynes, 1990).

In developing mouse embryos, FN is first expressed in blastocysts (Zetter and Martin, 1978; Wartiovaara et al., 1979; Thorsteinsdottir, 1992) and it has been suggested that FN may promote migration of parietal endoderm and trophoblast outgrowth during implantation (Armant et al., 1986; Grabel and Watts, 1987; Sutherland et al., 1988). During gastrulation, FN is expressed beneath the ectoderm at the position of prospective mesodermal migration in all vertebrate embryos examined (Hynes, 1990). In amphibian embryos, injections of antibodies to FN, or of reagents that inhibit integrin functions, completely block mesodermal migration and entry into the blastocoel (Thiery et al., 1985; Darribere et al., 1988; Johnson et al., 1992). In chicken embryos, anti-FN antibodies do not prevent delamination of mesodermal cells through the primitive streak but do block its lateral migration (Harrisson et al., 1993). Studies employing explant cultures as well as injections of antibodies and peptides also strongly implicate FN in neural crest migration in amphibians and birds (Thiery et al., 1985; Lallier and Bronner-Fraser, 1990; Hynes, 1990; Duband et al., 1991). FN has also been suggested to promote primordial germ cell migration (Heasman et al., 1981; ffrench-Constant et al., 1991), heart development, both in the formation of the primordia (Linask and Lash, 1986, 1988a,b) and in migration of cardiac cushion cells later in cardiac development (Mjaatvedt et al., 1987; ffrench-Constant and Hynes, 1988; Icardo et al., 1992), somitogen-

esis (Ostrovsky et al., 1983; Wedlich et al., 1989; Drake et al., 1991) and vasculogenesis (Risau and Lemmon, 1988; Risau, 1991).

In order to test the possible involvement of FNs in these various embryonic migrations and morphogenetic processes and in later events such as wound healing and oncogenesis, we have used homologous recombination in embryonic stem (ES) cells (Capecchi, 1989) to inactivate the FN gene and generate strains of mice deficient in FN. Analyses of embryonic defects arising in these strains support some of the proposed roles of FN but not others.

MATERIALS AND METHODS

Construction of the targeting vector

A 5′ rat FN cDNA probe was used to isolate a clone from a mouse genomic library from the MOV 13 strain (provided by D. Gray and R. Jaenisch, Whitehead Institute, M. I. T.). To construct a replacement-type gene targeting vector, a 6.2 kb *Eco*RI/*Sal* I (λ-derived) fragment including the FN 5′ exon and first three FN type I repeat exons was subcloned into Bluescript SK- (Stratagene). The *neo*/G418-resistance gene, under control of the mouse *PGK-1* promoter and *PGK* poly(A) addition site (McBurney et al., 1991), was isolated from plasmid pKJ1 by digestion with *Eco*RI and *Bgl*II and ligated between two *Sma*I sites in FN, leaving 0.8 kb 5′ flanking genomic DNA. This insertion results in replacement of 0.8 kb of the FN gene; deleting the translation initiation sequence and part of the signal sequence. The *PGK-tk* cassette (Rudnicki et al., 1992) was inserted into the *Hin*dIII and *Sal*I sites of the Bluescript polylinker, leaving 4.6 kb of FN gene between the *neo* and *tk* selection markers (Fig. 1A).

Growth, transfection and positive-negative selection of ES cells

The D3 line of ES cells (Doetschman et al., 1985, kindly provided by Dr Janet Rossant, Mt Sinai Hospital Research institute, Toronto,Ontario, Canada) was cultured in DMEM (high glucose) with 26 mM Hepes (pH 7.5), 14 mM sodium bicarbonate, 15 % fetal bovine serum (Hazleton), 1× non-essential amino acids (Gibco) and 0.1 mM β-mercaptoethanol. ES cells were maintained on a feeder layer of mitotically inactivated mouse embryonic fibroblasts at all times and medium was replaced daily. The neomycin-resistant feeders were prepared from embryos of a line of mice containing a neomycin-resistance transgene (gift of Dr. Rolf Kemler, Max-Planck-Institut fur Immunbiologie, Freiburg, Germany).

For transfection, 1.7×10^8 ES cells (our passage 4) were washed and resuspended in 6.4 ml HBS (25 mM Hepes (pH 7.1), 134 mM NaCl, 5 mM KCl, 0.7 mM Na_2P0_4) with 160 μg targeting vector DNA linearized at the 5′ end. The cell/DNA suspension was incubated on ice for 10 minutes and electroporated at 240 volts and 500 micro-Farads in a Gene Pulser (Biorad). Cells were incubated at room temperature for 15 minutes, pooled and plated on thirty 10 cm dishes containing G418-resistant feeder cells. After 36 hours, one dish was treated with G418 to determine transfection frequency. All other plates were treated with 200 μg/ml active G418 (Gibco) and 2 μM gancyclovir (a gift from Syntex Corporation). After 8 days of selection, the G418-alone plate had approximately 600 colonies. The double-selection plates combined had 223 colonies. Thus enrichment by gancyclovir selection, (number of G418-resistant colonies divided by the number of double-resistant colonies), is about 80-fold. All double-resistant colonies were picked and individually replated in 96-well dishes with feeder cells, allowed to re-attach for 14 hours and then split in half. After 1 day, one half of each colony was expanded further (without selection drugs) and the other was processed for DNA isolation (see below). After 2 more days, cells were passaged into 24-well dishes with feeders. 15 clones were determined as targeted by PCR (see below); one half of each targeted clone was frozen in 90% fetal bovine serum, 10% DMSO and one half was expanded without feeders for confirmation of homologous recombination (see below).

Blastocyst injection

Targeted ES cells were thawed to two 3.5 cm dishes with feeder cells and standard ES cell medium 2 days prior to blastocyst injection. Medium was replaced daily and 2 hours prior to trypsinization. One plate was trypsinized at the beginning of an injection session, and the second about 3 hours later. Trypsin (Gibco-BRL) was prepared fresh at 0.25% in 0.02% EDTA in PBS and prewarmed to 37°C. Cells were trypsinized, gently dispersed after addition of complete medium and pelleted. Cells were resuspended in ice-cold ES cell medium and kept on ice until transfer to the injection chamber.

Chimeras were generated essentially as described (Bradley, 1987). Briefly, 15-20 ES cells were injected into C57BL/6J blastocysts at E3.5. Embryos were allowed to re-expand for at least one hour after injection at 37°C, and then transferred to pseudopregnant CD1 recipients at 2.5 days postcoitum. 10-12 embryos were transferred to each recipient.

Analysis of DNA from ES cells, mice and embryos

ES cell DNA for PCR was isolated by resuspending a cell pellet in 55 μl 10% phosphate-buffered saline, freezing on dry ice and incubating at 95°C for 8 minutes. Lysed cells were incubated with 10 μg proteinase K (Boehringer Mannheim) at 55°C for 30 minutes, followed by 95°C for 8 minutes. PCR reaction conditions were essentially those described by the manufacturer of Taq polymerase (Perkin-Elmer Cetus) except that annealing of primers was at 55°C to increase specificity and 40 amplification cycles were performed. Oligonucleotide primers were as follows:

Neo gene: 5′-ATCGCCTTCTTGACGAGTTC-3′.
FN gene: 5′-GTAGTGTAGGAAGTCCAGAG-3′.

A 20 μl aliquot of each PCR reaction was electrophoresed on a 1.2% agarose gel, capillary-blotted to Zetaprobe (Biorad) and UV-crosslinked with a Stratalinker (Stratagene). A random-primed probe (Feinberg and Vogelstein, 1983) within the predicted amplification product (indicated in Fig. 1) was used to verify PCR products. Hybridization conditions were standard high stringency for nylon blots (Church and Gilbert, 1984).

To confirm homologous recombination, each clone was analyzed by Southern blot of genomic DNA. ES cells were lysed in 150 mM NaCl, 20 mM Tris-HCl (pH 7.5), 5 mM EDTA, 0.5 % SDS and 0.25 mg/ml Proteinase K (Boehringer-Mannheim) at 37°C for 30 minutes. Lysates were extracted once with phenol/chloroform, once with chloroform and ethanol-precipitated. DNA was digested with either *Bgl*II or *Hin*dIII. Gel electrophoresis, blotting and hybridization were as described above. The probe was 1.1 kb genomic DNA restriction fragment from outside the targeting vector (indicated in Fig. 1).

Mice were similarly genotyped by Southern blot. DNA from tail biopsies was isolated by proteinase K digestion followed by either phenol extraction and ethanol precipitation (Hogan et al., 1986) or isopropanol precipitation (Laird et al., 1991).

Cultured embryos and blastocysts were genotyped by separate PCR reactions. The mutant allele was assayed using the same primers as above, and the wild-type allele was assayed by replacement of the *neo* primer with a primer from genomic DNA that had been deleted in the targeting vector (5′-GTCTGTGCACACCA-GAGTGT-3′). DNA isolation, PCR conditions and Southern blotting were performed as for ES cells.

Whole-mount embryos were genotyped by Southern blot of DNA isolated from the yolk sac. Yolk sacs were quick-frozen in digestion buffer (Laird et al., 1991), followed by digestion with Proteinase K at 55°C for 2 hours. Lysates were extracted once with phenol/chloroform, once with chloroform and ethanol-precipitated.

Embryos in paraffin sections were genotyped by scraping embryonic tissue from sections. Scrapings from several sections were pooled in 60 μl H_2O, incubated with 20 μg Proteinase K at 55°C for 30 minutes, 95°C for 10 minutes. Separate PCR analysis with wild-type or mutant primer sets was described above. Maternal tissue was used for positive controls.

Quantitation of FN in plasma

Blood (0.5 ml) was drawn from anesthetized mice by heart puncture into a syringe containing 25 μl 0.2 M EDTA (pH 7.5). Plasma was separated from blood cells by centrifugation at 10 K revs/minute for 30 seconds and quick-frozen in small aliquots. All assays were performed on first-thaw aliquots. Concentration of FN in plasma was measured by radial immunodiffusion with an antibody to human FN (The Binding Site Inc.). Plasmas from 18 heterozygous and 13 wild-type animals were assayed.

Immunoprecipitation of FN from cultured embryos

Embryos were dissected from maternal tissue and yolk sac at E7.5. After washing in PBS and ES-cell medium, embryos were mechanically dissociated and cultured in gelatinized 24-well dishes with ES-cell medium (50% was conditioned on feeder cells) plus 1000 U/ml ESGRO (Gibco-BRL) and antibiotics. After 4 days, cultures were labelled in 90% ES-cell medium without methionine, 10% complete ES medium and 100 μCi/ml [^{35}S]methionine (New England Nuclear) for 24 hours. Immunoprecipitation of culture supernatants was performed in 10 mM EDTA, 2 mM PMSF, 2.2% ovalbumin, 100 mM Tris (pH 8.0), 0.1% SDS, 0.5% NP-40, 0.5% DOC. Primary antibody was either 10 μl rabbit anti-FN serum or 10 μl preimmune serum, for 1 hour at 37°C. Secondary antibody was 100 μl goat anti-rabbit IgG (Cappel), for 16 hours at 4°C. Precipitates were washed four times in excess detergent solution without ovalbumin. Total labelled supernatant and precipitates were denatured with 2% SDS, reduced with 0.1 M dithiothreitol and electrophoresed on 5% SDS-polyacrylamide gels (Laemmli, 1970).

Histology and immunofluorescence

Whole decidua were fixed in Carnoy's solution (60% ethanol, 30% chloroform, 10% glacial acetic acid) for 4 to 6 hours at 4°C, dehydrated through an ethanol series, cleared in xylene and embedded in paraffin. Each embryo was sectioned (8 μm) serially; adjacent sections were analyzed by immunofluorescence for FN, histological stain for morphology (haemotoxylin and eosin or toluidine blue, Polysciences) and PCR for genotype. To assay for FN, rehydrated sections were first blocked with 10% heat-inactivated goat serum (depleted of FN by gelatin-Sepharose gel filtration), 0.05% Tween 20, 0.02% azide in PBS for one hour. Rabbit anti-FN serum, diluted 1/100 in blocking buffer, was incubated with sections for 16 hours. Sections were washed in PBS, incubated in blocking buffer for 30 minutes, followed by incubation with FITC-conjugated goat anti-rabbit IgG (Cappel) at 1/200 dilution in blocking buffer, for 2 hours. All incubations were at 37°C. Sections were washed in PBS and mounted in Gelvatol with anti-fade.

RESULTS

Targeted disruption of the fibronectin gene in ES cells

The structure of the 5′ end of the mouse FN gene is shown in Fig. 1A. The 5′ exon encodes the signal, pro- and N-terminal sequences and exons I-1, I-2 and I-3 encode the first three FN type I repeat units. To obtain targeted disruption of the FN gene, we used positive-negative selection (Mansour et al., 1988; see Materials and Methods). In the targeting vector, Fig. 1A, the FN gene was disrupted by deletion of 0.8 kb between two *Sma*I sites near the 5′ end removing the translation initiation codon and part of the 5′exon.

Linearized targeting vector was transfected into ES cells by electroporation. After 8 days selection, double-resistant colonies were picked and expanded. Double-resistant clones were initially screened for homologous recombination by Southern blot analysis of polymerase chain reaction (PCR) products in pools of 12, using primers as shown in Fig. 1A. Of the nineteen pools screened, nine contained the predicted amplification product and were individually reassayed. Fifteen targeted clones were identified and all were confirmed by Southern blot analysis of genomic DNA with two restriction enzymes (*Hin*dIII and *Bgl*II, Fig. 1A). Fig. 1B shows results from this analysis for the four targeted clones that were used to make chimeric mice. These data show that homologous recombination frequency at the 5′ end of the FN gene is at least 1 targeted clone per 1200 G418-resistant transfectants (15/18,000) or 1 targeted clone per 15 double-resistant transfectants (15/223). All targeted clones were tested for additional random insertions by probing genomic DNA with *neo* sequences. All clones had a single hybridizing band at the size predicted for a single *neo* insertion in the FN gene (not shown).

Generation of mice heterozygous for the targeted FN allele

To generate mice harboring the targeted FN allele, four randomly chosen targeted ES cell clones were injected into C57BL/6J blastocysts. Extensive ES-cell contribution was observed with all four clones, as assayed by coat color chimerism (30-90%). All chimeric males were mated to C57BL/6J females and offspring scored for coat color. Of the four targeted ES cell clones injected, three contributed to the germ line of chimeric males, resulting in pups with agouti coat color. Inheritance of the targeted FN allele was determined by Southern blot analysis of DNA isolated from tail biopsies. Of the 148 agouti progeny genotyped, 71 were heterozygous and 77 were wild-type. Fig. 1C shows this analysis for all agouti pups from two litters from one germline chimera.

Mice heterozygous for the targeted FN allele appeared healthy and were approximately the same size as their wild-type littermates. Viability, to at least two years, and fecundity were also normal. However, the concentration of FN in the blood plasma was one half that of wild-type littermates. Mean concentration of FN in wild-type mice was 580 μg/ml (s.d. 113) while that in heterozygous littermates was 233 μg/ml (s.d. 65).

Homozygosity for the targeted allele results in early embryonic lethality

Heterozygous mice were intercrossed and progeny assayed by Southern blot analysis of tail DNA at three weeks after birth (P21) and of embryos at E14.5. No homozygous embryos or pups were detected, indicating that homozygous

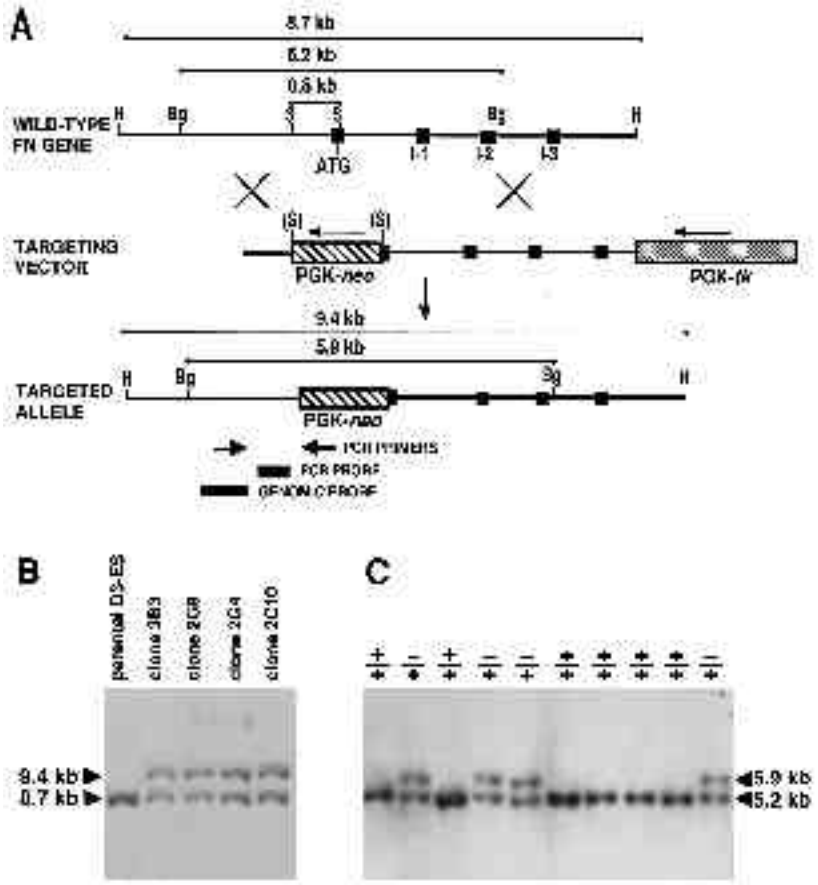

Fig. 1. Targeted inactivation of the fibronectin gene in ES cells and mice. (A) Wild-type FN gene, targeting vector and targeted allele. FN exons I-1, I-2 and I-3 encode the first three FN type I repeats. The PGK-*neo* cassette was inserted between two *Sma*I sites replacing parts of the promoter region and first exon. PCR primers and probe used to detect the amplification product are indicated; arrows indicate orientation of selectable markers. (B) Southern blot analysis of double-resistant ES cells. Homologous recombination of the targeting vector with a wild-type FN allele was confirmed with the probe indicated outside the targeting construct. A novel 9.4 kb *Hin*dIII fragment was generated by deletion of 0.8 kb of genomic DNA and insertion of the 1.5 kb PGK-*neo* selection cassette in the targeting vector. (C) Southern blot analysis of agouti progeny of a germ-line chimera. A novel 5.9 kb *Bgl*II fragment was detected with the same probe as in (B). S, *Sma*I; Bg, *Bgl*II; H, *Hin*dIII.

embryos die earlier in gestation. These results are pooled from the three targeted clones that contributed to the germ line and include progeny from both intraclonal and interclonal crosses. The lethality can therefore be attributed to the targeted mutation.

To characterize the embryonic lethality, we have genotyped embryos from heterozygous matings at several stages by PCR analysis of blastocysts or of paraffin sections or by Southern blot of yolk sac DNA. These data are summarized in Table 1; stage descriptions apply to normal embryos at a particular age. Preimplantation and early postimplantation homozygous mutant embryos were recovered at the expected frequency. Beginning at E8.0, homozygotes appeared developmentally delayed and abnormal (see below). By E9.5, wild-type and heterozygous littermates had 20-25 somites and had turned completely. In contrast, homozygous mutant embryos appeared to be deteriorating. By E10.5, some homozygous mutants were still detectable but deterioration was more pronounced. Therefore, the targeted mutation is a recessive embryonic lethal.

Table 1. Progeny of FN$^+$/FN$^-$ × FN$^+$/FN$^-$

	Stage	Assay	+/+	+/−	−/−
E3.5	Blastocysts	PCR	18	28	13
E7.5	Advanced primitive streak	PCR	8	12	9†
E8.0	Early headfold, unturned, 4-5 somites	PCR	8	18	5*
		Southern	3	4	4*
E8.5	Turning, 8-12 somites	PCR	6	9	5*
		Southern	21	37	15*
E9.5	Turned, 20-25 somites	PCR	1	3	1*
		Southern	4	7	5*
E10.5	Appendages forming	Southern	1	2	3*
			70	120	60
E14.5	Finger separation, over 60 somites	Southern	7	12	0
P21	Pups	Southern	70	112	0

*Embryos appeared abnormal.
†For three of these embryos, genotype was inferred from anti-FN staining.

Cultures of homozygous targeted embryos do not secrete FN

At E7.5, embryos from heterozygous matings were dissected, mechanically dissociated and cultured. After four days, cultures were exposed to [^{35}S]methionine for 24 hours. Labelled culture medium was assayed for presence of newly synthesized, secreted FN by immunoprecipitation. Genotypes of cultured embryos were determined by PCR of the cultured cells after removal of labeled media. Of the 21 embryos assayed, 6 were wild type, 11 were heterozygous and 4 were homozygous. In Fig. 2, autoradiograms of total culture media and immunoprecipitated material are shown for a representative subset of the embryos assayed. The protein profile of total culture media from individual

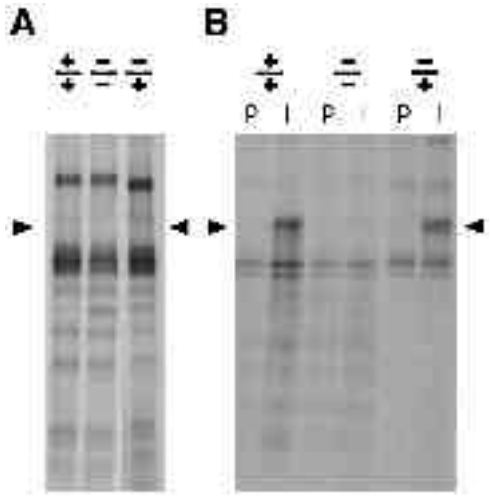

Fig. 2. The targeted mutation is a true null allele. E7.5 embryos from heterozygous matings were mechanically dissociated and cultured individually. Newly synthesized FN was assayed by labelling with ^{35}[S]methionine and immunoprecipitation of the culture supernatant. Embryonic genotype is above each lane. (A) Autoradiograph of total culture supernatants showed comparable incorporation of label. (B) Autoradiograph of immunoprecipitated material. FN migrated as a single band at 230×10^3 M_r and was absent from cultures derived from homozygous targeted embryos. P, preimmune serum; I, anti-FN serum; +/+, wild-type; +/−, heterozygous; −/−, homozygous mutant.

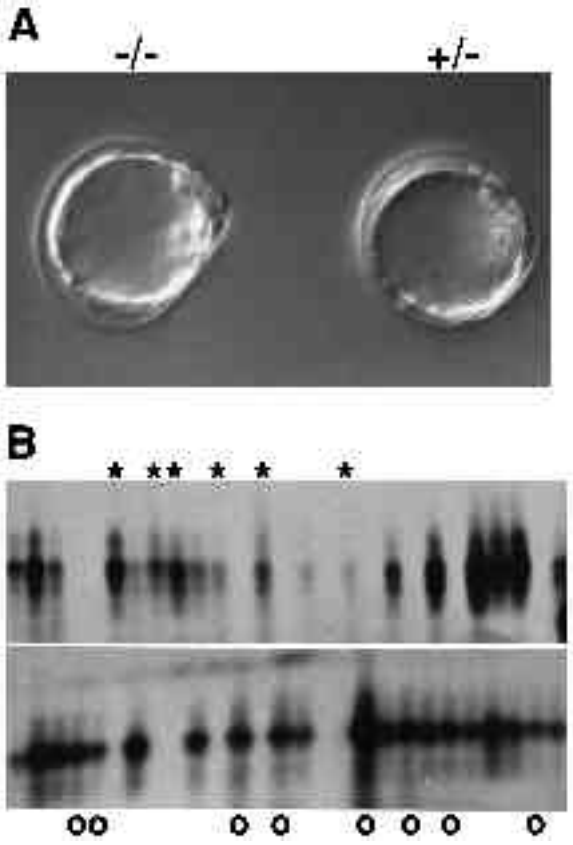

Fig. 3. Preimplantation *FN.null* homozygotes appear normal. Blastocysts were photographed and genotyped by PCR. (A) Like its heterozygous littermate, a homozygous *FN.null* blastocyst has expanded and is hatching from the zona pellucida. (B) DNA from each blastocyst was assayed by PCR for presence of the wild-type (lower panel) and the *FN.null* (upper panel) alleles. Amplification products were detected by hybridization with an internal probe. Genotype is indicated above or below each pair of lanes for homozygous blastocysts only: ◯, wild type; ***,** mutant.

embryos indicated that growth was reasonably comparable between cultures (Fig. 2A). Microscopic examination of cell-type heterogeneity and proliferation also suggested equivalence between cultures. In wild-type and heterozygous cultures, FN was a single broad band at 230×10^3 M_r which was absent in immunoprecipitations with preimmune serum (Fig. 2B). In contrast, FN was not detectable in immunoprecipitations from cultures of homozygous targeted embryos. Thus, the targeted FN mutation is indeed a true null allele, which we will refer to as *FN.null.*

FN.null homozygous embryos implant and initiate gastrulation

To determine whether *FN.null* homozygous preimplantation embryos were normal, 59 blastocysts (E3.5) were photographed and genotyped. Homozygous *FN.null* blastocysts appeared normal (Fig. 3A) and were detected at expected frequency (Fig. 3B). Like normal littermates, homozygous *FN.null* blastocysts expanded to the expected size and then hatched from the zona pellucida within one day in culture.

Littermates from heterozygous crosses at E7.5 were compared by assay of three parameters: genotype, FN accumulation and morphology. To determine the genotype of sections, embryonic material was scraped from slides and subjected to PCR. Of the 29 E7.5 embryos assayed, genotypes were observed in the expected ratios (Table 1). Fig. 4 compares wild-type and mutant embryos that have been stained with a polyclonal anti-FN serum. In wild-type embryos (Fig. 4A,D), FN is localized between the three germ layers as well as among the mesodermal cells, while the ectoderm and endoderm appear to lack FN. At this stage, the embryo has not yet undergone the process of turning, so the ectoderm is on the inside, surrounding the amniotic cavity (Kaufman, 1992). Extraembryonic tissues also contain FN, which is localized between the ectodermal and mesodermal cell layers of the amnion and in the early blood islands of the yolk sac. This distribution of FN immunoreactivity is in agreement with previous reports (Wartiovaara et al., 1979).

In *FN.null* homozygotes (Fig. 4B,E), both embryonic and extraembryonic FN are absent. Maternal FN in the decidual tissue serves as a positive control for anti-FN staining. Upon histological staining of serial sections (Fig. 4C,F), *FN.null* homozygotes appeared reasonably normal, but somewhat smaller than normal littermates. Mutant embryos had three germ layers, apparently normal extraembryonic membranes, except for a concave amnion, and normal cellular morphology at the light microscopic level. The trophoblastic giant cells (the embryonic cells most intimately involved in uterine implantation) also appeared normal in the *FN.null* homozygotes, with respect to morphology, number and distribution. Comparison of embryos in transverse orientation

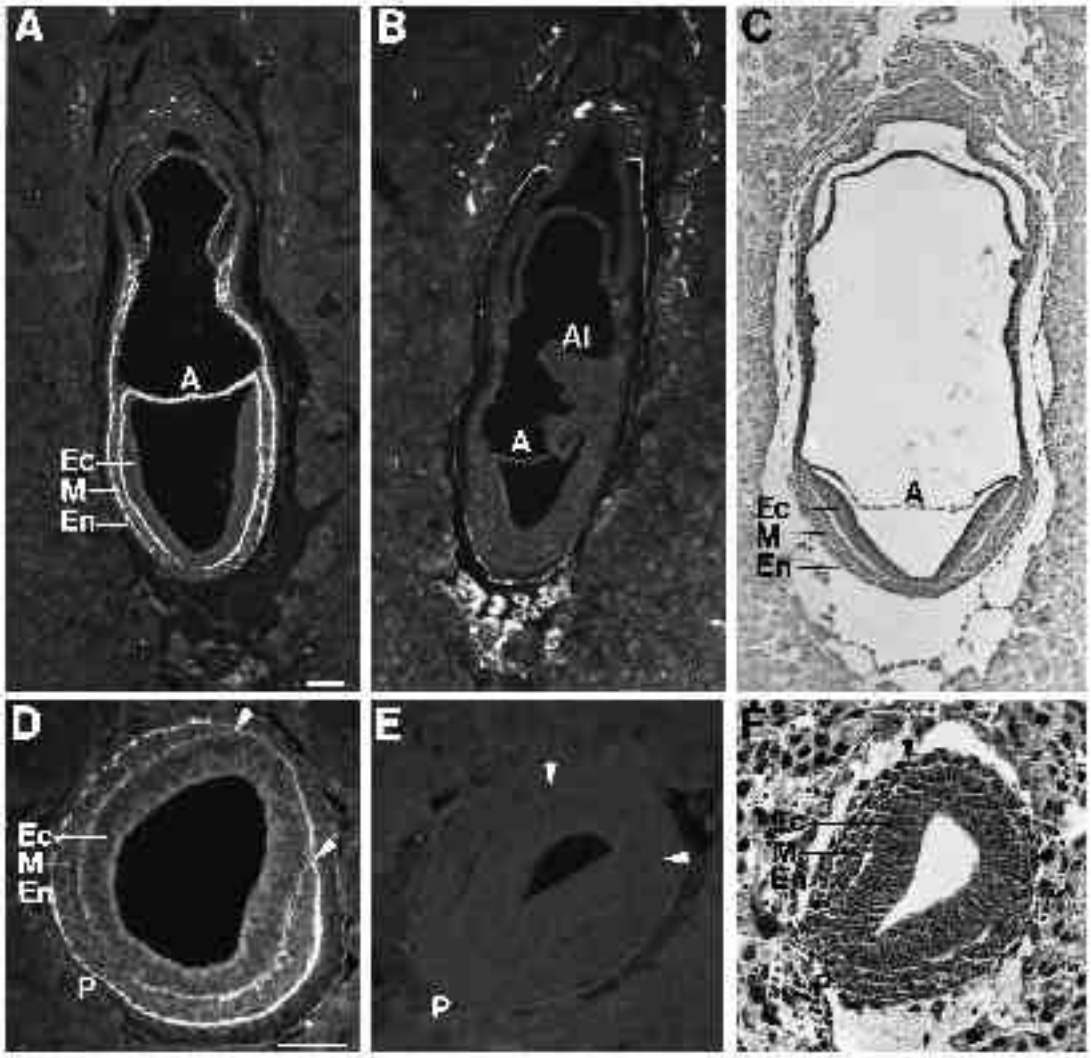

Fig. 4. Postimplantation *FN.null* homozygotes lack FN, yet have three germ layers. E7.5 advanced primitive streak embryos were sectioned either sagittally or transversely while in the maternal deciduum, stained with anti-FN, genotyped by PCR or stained histologically. In normal embryos (A), FN was localized between the three germ layers of the embryo as well as among the mesodermal cells. FN was also detected between cell layers in the amnion and yolk sac. In contrast, homozygous mutant embryos (B) had no FN staining within the embryo; staining was detected in the maternal tissue only. The fluorescence signal in Reichert's membrane is not due to specific staining. Histological staining of mutant embryos with toluidine blue (C) showed that the expected three germ layers and extraembryonic membranes were all present. Transverse sections show lateral movement of mesoderm from the primitive streak in a normal embryo stained with anti-FN (D), a FN-negative embryo (E) and a FN-negative embryo stained with hematoxylin and eosin (F). Ec, embryonic ectoderm; M, embryonic mesoderm; En embryonic endoderm; P, primitive streak; Arrowhead, extent of lateral spread of mesoderm; A, amnion; Al; allantois; bars, 100 μm.

(Fig. 4D-F) showed a distinct primitive streak and significant lateral movement of mesodermal cells from the streak had occurred in FN-negative embryos. We sectioned and examined nine *FN.null* homozygous embryos at E7.5 and all appeared similar.

Embryonic abnormalities appear after gastrulation begins

To determine the nature of the defects in *FN.null* embryos at later stages of development, we assayed embryos of various ages for genotype, FN accumulation and morphology. By E8.0, abnormalities were beginning to appear in the homozygous *FN.null* embryos. In normal embryos at E8.0 (early head-fold stage), a mid-line sagittal section (Fig. 5A) shows FN localized in the underlying mesoderm of the head-fold, the primitive heart and the allantois. A paraxial sagittal section (Fig. 5B) shows FN surrounding the somites and between the ectodermal and mesodermal cell layers of the amnion; FN is also present in the blood islands of the yolk sac. Homozygous mutant embryos lacked FN staining, as at day E7.5 (not shown). Comparison of histologically stained E8.0 embryos (Fig. 5C,D) shows the morphological abnormalities observed in the *FN.null* homozygous embryos. These abnormalities are consistent with the slight defects observed in E7.5 homozygotes. Mutant embryos had a shortened anterior-posterior axis compared to normal

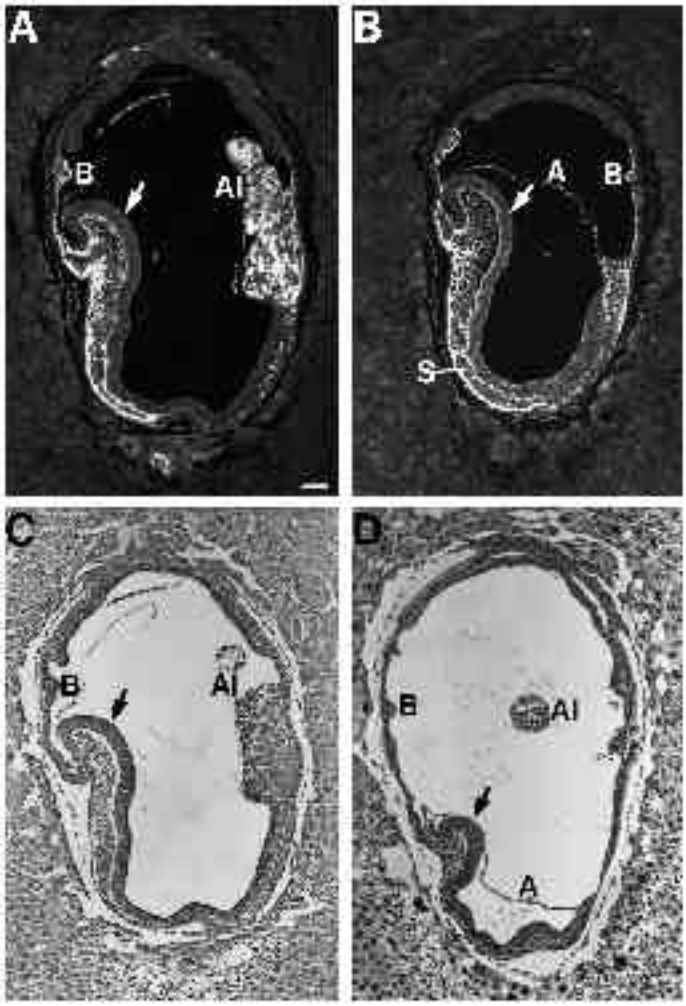

Fig. 5. E8.0: distortions appear in *FN.null* homozygotes. In mid-sagittal (A) or para-sagittal (B) sections of a normal early headfold-stage embryo, FN was localized in the headfold mesoderm, surrounding the somites, between the cell layers of the amnion, within the allantois and the blood islands of the yolk sac. Histological comparison of a normal embryo (C) with a *FN.null* homozygote (D) showed a shortened anterior-posterior axis, distortions in neural ectoderm, a deficit of headfold mesoderm and a concave amnion. Arrow, headfold with underlying mesoderm; S, somite; Al, allantois; A, amnion; B, blood island; bar, 100 μm.

embryos at the same stage and the head and trunk mesoderm were deficient. The ectoderm of mutant embryos had multiple bends and distortions. Paraxial serial sections (not shown) of mutant embryos lacked somites, but had normal allantois and yolk sac including apparently normal blood islands. The amnion was closely apposed to the embryo, as compared with the normal amnion in Fig. 5B and appeared as if there was a deficit in pressure in the amniotic cavity. We observed the same abnormalities in all five E8.0 homozygous *FN.null* embryos analyzed by sectioning. We also compared whole-mount preparations of four dissected progeny at E8.0 (not shown). The same abnormalites were observed as in sectioned embryos, except that extraembryonic membranes were not assayed.

Further abnormalities became evident when we examined progeny of heterozygous matings at E8.5. Genotypes were determined either by Southern blot analysis of yolk-sac DNA or by PCR of sectioned material. Whole-mount analysis of embryos in Fig. 6 shows two extremes in severity of phenotype that we observed in *FN.null* homozygotes. In Fig. 6A, littermates are presented in dorsal view; two mutant embryos flank a normal embryo. The anterior-posterior axis of the mutant embryos was greatly shortened compared with the normal littermate at this stage. The head-folds had remained small and distorted. The neural tube was also abnormal in mutant embryos. Rather than the straight closure observed in the trunk region of normal embryos, mutant embryos had a kinked neural tube. While normal embryos at this stage have between 8 and 12 pairs of somites, *FN.null* homozygotes lacked somites. Lateral view of these two mutant embryos (not shown) revealed that no primitive heart bulge was visible. Fig. 6B shows comparison of a less severely abnormal mutant embryo with a normal littermate. Note that the normal embryo had distinct somites, a prominent primitive heart and was in the process of turning. In the mutant embryo, the shortened anterior-posterior axis, lack of somites and kinked neural tube were evident. However, this mutant embryo was scored as less severe, compared with those in Fig. 6A, because the head folds were larger and less distorted, the anterior-posterior axis was less shortened and a primitive heart bulge and optic cup were observed. Some of the mutant embryos at this stage had a beating heart. Of the 20 embryos examined at E8.5, 13 had a visible primitive heart whereas the rest did not. None of the mutant embryos had initiated turning. Neither extreme of phenotype was associated with a particular targeted clone, and we also observed this heterogeneity in progeny from intercrosses between targeted clones (see Discussion).

Mesodermal defects are accentuated as development proceeds

Histological analysis of sectioned E8.5 *FN.null* homozygous embryos revealed additional embryonic and extraembryonic defects. For comparison, Fig. 7 shows sections of normal E8.5 embryos, which are in the process of turning. FN is widely distributed in the embryo; it is found in the head mesenchyme and the heart and surrounding neural tube, notochord, somites and dorsal aortae. FN is also prominent in the extraembryonic membranes including the blood islands. As at earlier stages, homozygous mutant embryos showed no staining for FN (data not shown) and were examined by haemotoxylin-eosin staining. Fig. 8 shows sections from embryos with the two extremes of phenotype that we observed. Fig. 8A,B shows sections of two embryos of the less severe phenotype, in sagittal and coronal orientations respectively. Fig. 8C-F shows a series of transverse sections along the anterior-posterior axis of one mutant embryo, which is representative of the more severe phenotype.

As at earlier stages, all mutant embryos had a shortened anterior-posterior axis in comparison with normal embryos. The head folds were also abnormal, but in Fig. 8A to a lesser extent; an optic cup had begun to form. In the more severely abnormal embryos (Fig. 8C), the headfolds were small and misshapen, with a deficit in mesenchymal cells in the underlying mesoderm. Many mesodermal cells were pycnotic, as

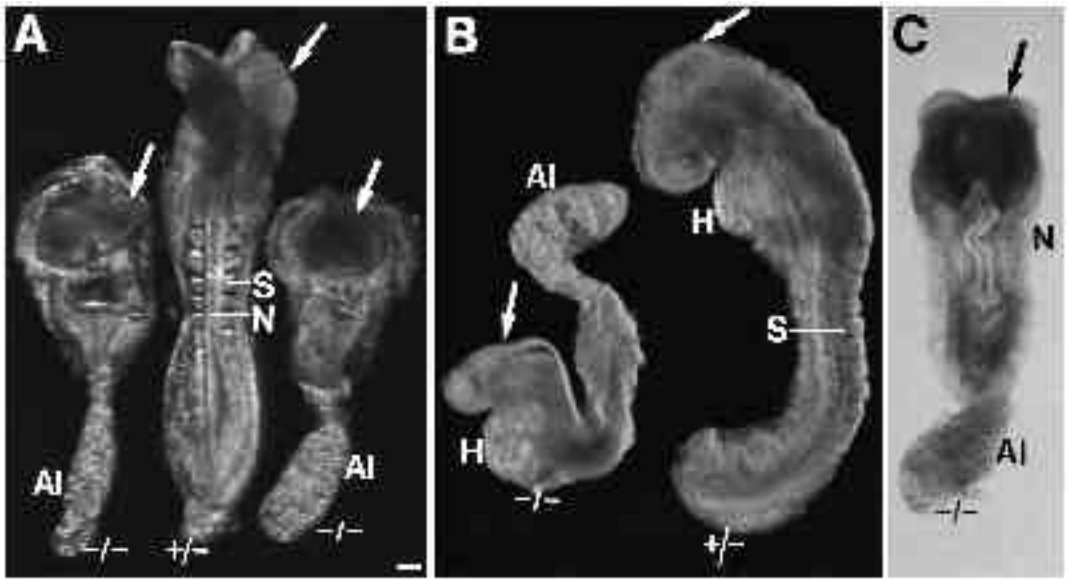

Fig. 6. E8.5: *FN.null* homozygotes continue to develop, but defects become more pronounced. (A) Dorsal view of two homozygous mutant embryos showed shortened anterior-posterior axis, undersized, distorted headfolds and kinked neural tube. In side view (not shown), the same embryos had no somites or heart bulge. (B) Side view of a third homozygous mutant littermate showed some of the same defects, while others appeared less pronounced; note the primitive heart bulge. In dorsal view (not shown), the neural tube was kinked. (C) Dorsal view of another homozygous mutant that also displayed somewhat less pronounced defects and showed kinked neural tube. In side view (not shown), somites were absent, but a heart bulge was observed. All homozygotes were developmentally delayed because they had not initiated turning and the allantois had yet not fused with the chorion. −/− homozygous *FN.null* embryo; +/− heterozygous littermate; arrow, headfold; N, neural tube; S, somite; H, heart; Al, allantois; bar, 100 μm.

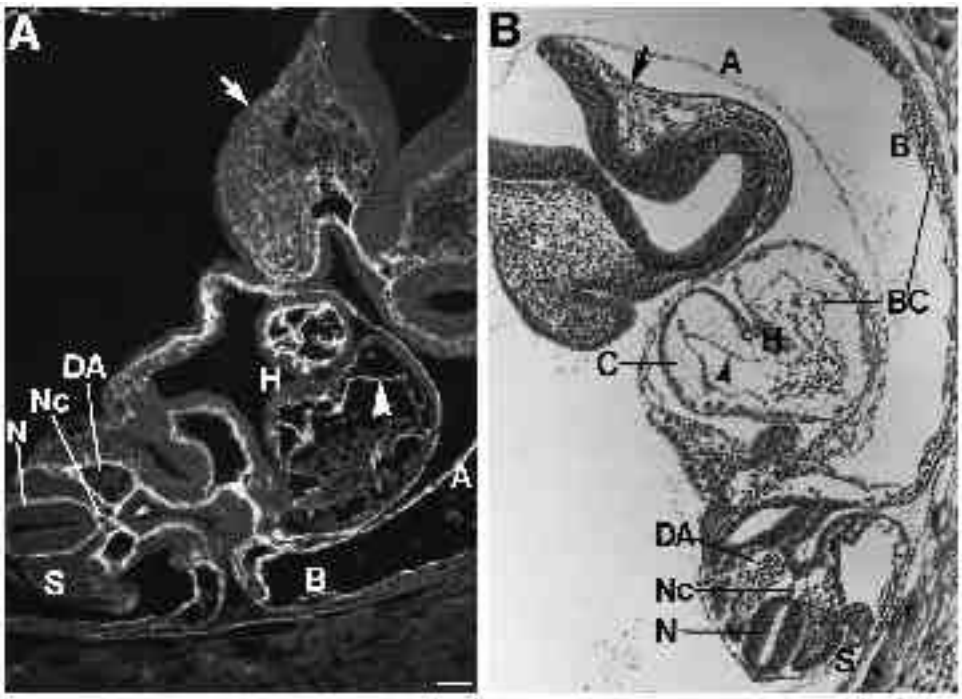

Fig. 7. E8.5: distribution of FN in normal embryos. In normal E8.5 embryos, embryonic and extraembryonic vasculatures have fused, and primitive red blood cells are present in the heart and dorsal aortae as well as in the yolk-sac vasculature. (A) A normal embryo, in the process of turning, stained with anti-FN. FN was detected within the head mesenchyme, surrounding the notochord, neural tube, somites and dorsal aortae, in the endocardium, between the cell layers of the amnion and in the blood islands of the yolk sac. (B) Histological analysis of a normal embryo of similar stage. Arrow, head mesenchyme; H, heart; arrowhead, endocardium; C, cardiac jelly; BC, primitive red blood cells; DA, dorsal aorta; Nc, notochord; N, neural tube; S, somite; A, amnion; B, blood island; bar, 100 μm.

were some in the neural tube. The neural tube appeared kinked for its entire length in whole-mount analysis. In some embryos, the kinks were in parallel on the two sides and the neural tube appeared to close normally in some regions. Fig. 8D,E illustrates this property in section; in the trunk region, the neural tube was closed but, further posterior, it appeared open and very kinked. In a sagittal section of the most advanced embryo observed (Fig. 8A), the neural tube bent in and out of the plane of section.

Heart development was also abnormal in the E8.5 *FN.null* embryos. In the most severely abnormal embryos, heart primordia had not fused and were positioned laterally (Fig. 8C). In normal embryos at this stage even prior to fusion, the primordia are closely apposed at the mid-line (Kaufman and Navaratnam, 1981). In the more advanced, less severely defective mutant embryos, the heart primordia had fused, but their morphology was abnormal. Compared with normal embryos, the mutant myocardial tissue appeared thickened,

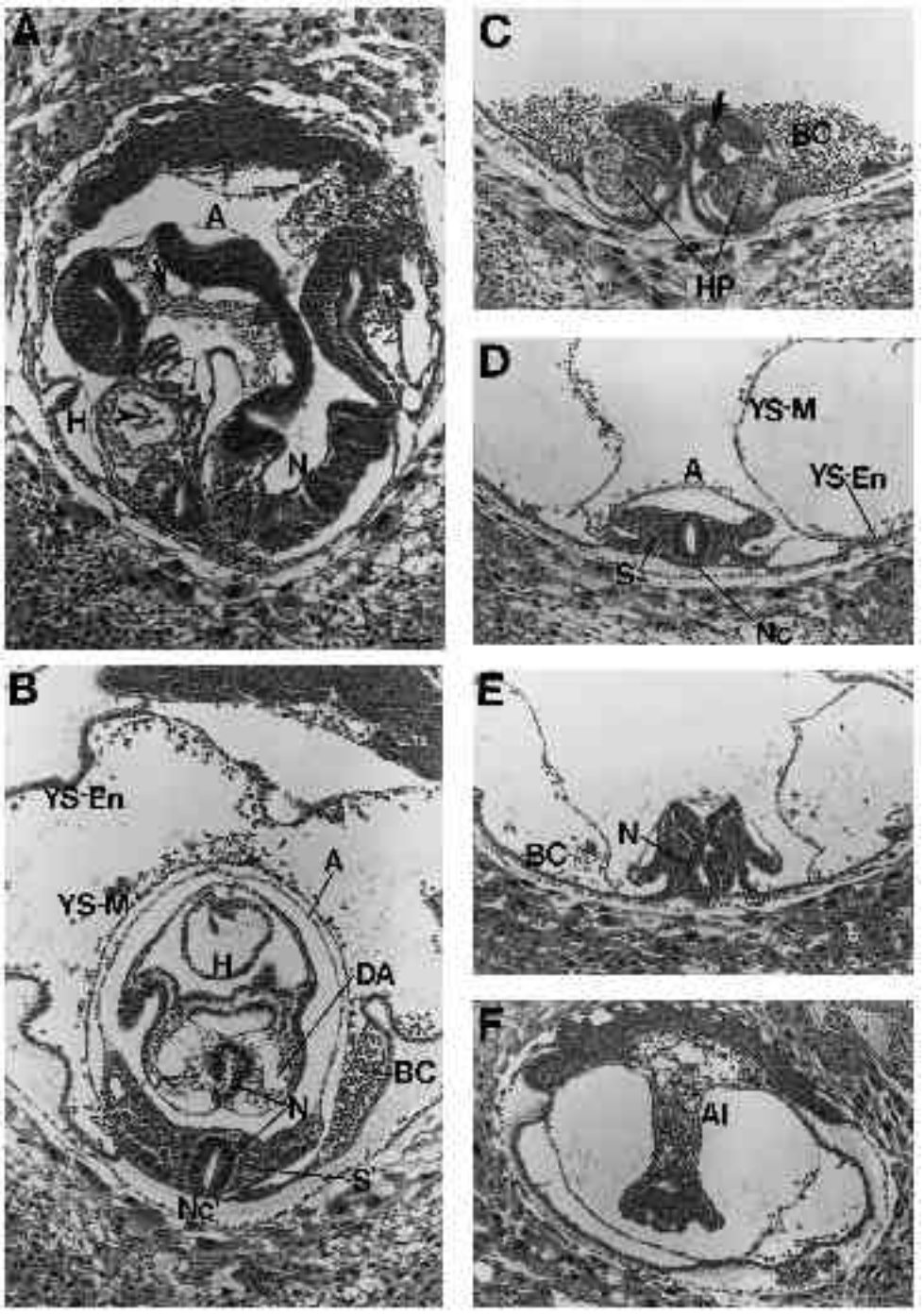

Fig. 8. E8.5: histological analysis detects additional embryonic and extraembryonic defects in *FN.null* homozygotes. (A) Sagittal section of the most advanced *FN.null* homozygous embryo observed. Although a heart was present, its morphology appeared abnormal; myocardium was thickened and cardiac jelly was deficient. The kinked neural tube passed in and out of the plane of section. Somites were absent. Head mesenchyme was deficient. Relatively few primitive red blood cells were observed in the embryonic vessels. (B) Transverse section of a different *FN.null* homozygous embryo; embryonic vessels appeared distended and the heart lacked a distinct endocardium. Both heart and vessels contained relatively few blood cells. The mesodermal and endodermal layers of the yolk sac were separate, and no blood islands were observed. Instead, blood cells were widely dispersed between the separate layers. Notochord and somites were not detectable and the neural tube contained many pycnotic cells. (C-F) Non-adjacent serial sections along the anterior-posterior axis of a more severely defective *FN.null* homozygous embryo, showing additional defects. (C) Headfolds were small and distorted, with a deficit in underlying mesoderm, and contained many pycnotic cells. Primitive heart primordia had not fused. Amnion appeared undersized and closely apposed to the embryo. Blood cells were found in the exocoelomic cavity rather than in the yolk sac vasculature. (D) Organized notochord and somites were absent, and lateral mesoderm was deficient. Layers of the yolk sac were separated rather than organized as the yolk sac vasculature. Amnion again appeared undersized and in close contact with the embryo. (E) Neural tube was kinked. Dorsal aortae were absent. (F) Allantois appeared to fuse normally with the chorion. Arrow, headfolds with underlying mesoderm; H, heart; arrowhead, endocardium; HP, heart primordium; N, neural tube; DA, dorsal aortae; Nc′, normal location of notchord; S′, normal position of somites; A, amnion; BC, primitive red blood cells; YS-En, endodermal component of the yolk sac; YS-M, mesodermal component of the yolk sac; Al, allantois.

cardiac jelly was deficient and endocardium was either abnormal in morphology (Fig. 8A), not distinguishable from a thickened myocardium or absent (Fig. 8B). In normal embryos at this stage, the heart is often densely packed with primitive red blood cells (Fig. 7B); in contrast, the hearts of mutant embryos, even when present, had few if any blood cells (Fig. 8A,B).

Mesodermal abnormalities were also observed in the trunk region of all mutant embryos. In normal embryos, the notochord is detected as a small, organized group of darkly

staining cells on the ventral side of the neural tube (Fig. 7B). In *FN.null* mutant embryos, however, no organized notochord was distinguishable. Instead, the endodermal lining of the prospective midgut appeared juxtaposed to the neural tube (Fig. 8B,D,E). Organized somites, which would normally flank the neural tube and notochord (Fig. 7B), were also not distinguishable in the mutant embryos (Fig. 8A-E). However, condensations of cells suggestive of incipient somites were observed in 3 of the 20 E8.5 mutants examined.

Defects also occur in extraembryonic membranes and vasculature

The amnion appeared normal in some respects; the ectoderm and mesoderm components were present and closely apposed. Compared to a normal amnion, however, the mutant amnion was smaller and located very close to the headfolds (Fig. 8C), the trunk region (Fig. 8D) and also the posterior end (Fig. 8E). This amnion defect was also observed in the less severe embryos (Fig. 8A,B).

The mutant yolk sac was also defective. In normal embryos, the mesodermal component of the yolk sac has blood islands that contain primitive, nucleated red blood cells. At this stage, the blood islands are normally fusing to form the yolk sac vasculature (Fig. 7B). In the mutant embryos, however, the two layers of the yolk sac (endoderm and mesoderm) appeared to split apart (Fig. 8B-F). Primitive blood cells, rather than remaining confined to blood islands and vessels, had accumulated as a pool in the exocoelomic cavity. These cells were also observed in the area between the separated mesodermal and endodermal components of the yolk sac (Fig. 8B,D-F). The mesodermal component of the yolk sac often appeared undersized and located abnormally close to the embryo compared to the endodermal component (Fig. 8B,D,E). This yolk sac defect was also evident on dissection of embryos from the deciduum. The embryonic vasculature was also defective in the mutant embryos. Dorsal aortae, which contain blood cells in normal embryos at this stage (Fig. 7B), were absent in embryos that also displayed the most delay in heart development (Fig. 8C-E). In embryos with a more advanced heart, dorsal aortae were present but were abnormal and distended (Fig. 8B) and contained few blood cells.

In summary, the *FN.null* embryos proceed normally through implantation and initiate gastrulation, including significant mesodermal movement. Defects in a variety of systems are subtle at E7.5 but develop progressively from day E8.0 on. Extensive mesodermal dispersion occurs, although many of the defects can be explained in terms of deficits in mesoderm (see Discussion). Some structures normally rich in fibronectin fail to develop (notochord, somites) while others (amnion, yolk sac, blood islands) initially develop normally. Failures in development of both embryonic and extraembryonic vasculatures are a likely cause of the degeneration of the embryos after day E8.5. Heterogeneity in mutant phenotype was particularly noticeable in heart development but was also noted in development of blood vessels and extent of the neural folds.

DISCUSSION

The null mutation that we have generated in the FN gene is a recessive embryonic lethal mutation in three independent strains and in intercrosses among these strains. These results prove the importance of FN for successful completion of embryogenesis. However, the details of the phenotypic defects in the homozygous mutant embryos conform with only some of the predictions based on in vitro analyses or earlier intervention experiments in embryos.

Although FN is expressed in preimplantation blastocysts (Zetter and Martin, 1978; Wartiovaara et al., 1979; Thorsteinsdottir, 1992; our unpublished data) we observe no defects in *FN.null* blastocysts (Fig. 3), which hatch and implant at normal frequency (Table 1). If FN is indeed involved in implantation or parietal endoderm migration, then maternal FN can suffice. Maternal mRNA for FN, as in amphibians (Lee et al., 1984; Darribere et al., 1984), is a possibility, although unlikely. More likely is a contribution of maternal decidual FN, which is widely expressed (Fig. 4; Wartiovaara et al., 1979; Rider et al., 1992). Alternatively, other matrix proteins may substitute for FN in the mutant embryos. In any case, our results provide no support for a crucial role for blastocyst FN.

Even more surprising is the fact that the *FN.null* embryos appear to initiate gastrulation (Fig. 4) in the complete absence of embryonic FN (Figs 2, 4). This is in marked contrast with the results of experiments on amphibian embryos in which injection of antibodies to FN completely blocks mesoderm ingression (involution) and migration (Boucaut et al., 1984; Johnson et al., 1992). In the *FN.null* mouse embryos, mesoderm not only forms but also appears to spread significantly between the ectodermal and endodermal layers (Figs 4, 5). Results on chicken embryos are intermediate; injection of anti-FN into the space between the epiblast and hypoblast does not block ingression (delamination) of mesodermal cells from the primitive streak but prevents lateral migration (Harrisson et al., 1993). Circumferential movement around the cylindrical mouse embryo is equivalent to lateral movement in the discoid chicken embryo and it clearly proceeds in the absence of FN, as shown by transverse sections of E7.5 embryos (Fig. 4E,F) and by the presence of head mesenchyme at E8.0 (Fig. 5D). Mesodermal cells also emerge from the primitive streak into the amnion, chorion, yolk sac and allantois (Figs 5-8) although there may be some later deficits (see below). Clearly mesodermal movement in the mouse is not totally dependent on FN. One possibility that needs further investigation is that other matrix molecules are upregulated in response to the absence of FN in the mutant embryos. Such upregulation presumably does not occur in the shorter term antibody injection experiments in avian and amphibian embryos.

While only subtle defects appear at the beginning of gastrulation in the *FN.null* embryos, deformities rapidly develop from E8.0 onwards and the mutant embryos deteriorate during the tenth and eleventh days of gestation. The low number of primitive blood cells in the embryonic vasculature may reflect a defect in the fusion with the extraembryonic vasculature. Alternatively, the large size of embryonic vessels and lack of the extraembryonic vessels may prevent generation of sufficient pressure in the cardiovascular system to move blood into the embryo, with consequent deterioration at later stages. The later stages of dete-

rioration are not interpretable because of this lack of a normal vasculature, which should develop by E8.5 (Kaufman, 1992). However, the defects visible at E8.0 and E8.5 can be interpreted in terms of a deficit in mesoderm. Mutant embryos show shortened anterior-posterior axes, fail to develop certain mesodermally derived structures (notochord, somites) and develop others (heart, blood vessels) variably and abnormally (Figs 5-8). There appears to be a general deficiency in mesoderm. Thus, the quantity of head mesenchyme appears reduced (Figs 5D, 8C), lateral mesoderm flanking the neural tube is reduced in amount and, as mentioned, somites and notochord are absent (Figs 6, 8). Although extraembryonic mesoderm is clearly present in the amnion and yolk sac, these membranes later develop abnormally and one interpretation of the defects is a deficiency of mesoderm (qualitative or quantitative). Thus, while the amnion initially forms normally (Fig. 4B,C), it later becomes tightly apposed to the embryo as if it has failed to expand in area (Fig. 5D, 8). Similarly, although the yolk sac initially forms normally, including the development of blood islands (Fig. 4C, 5D), the mesodermal layer later separates from the endodermal layer and retracts towards the embryos, again as if it has failed to increase in area or is defective in cell adhesion (Fig. 8). Both blood cells and vascular endothelial cells are mesodermally derived and, while primitive red blood cells do develop (Fig. 8), blood vessels do not, strongly suggesting a role for FN in vasculogenesis (cf. Risau, 1991). The normal development of primitive red blood cells in the absence of FN shows that a FN matrix is not required for erythropoiesis as has been suggested for erythroleukemia cells (Patel and Lodish, 1987).

The kinked neural tube, which is a characteristic feature of the mutant embryos (Figs 6, 8), may be a secondary defect, although the presence of FN surrounding the neural tube in normal embryos (Fig. 7A; Martins-Green, 1988) might also suggest a direct effect. The absence of notochord and somites and reduced amount of mesoderm flanking the neural tube could all represent loss of support for the neural tube leading to its deformation. Alternatively, the failure of the embryonic axis to elongate normally could lead to kinking of the neural tube if it continues to elongate, as reported for *curly tail* (ct) mutant embryos (Copp et al., 1988; Brook et al., 1991). The necrosis of some cells in the neural tube (Fig. 8B) could be a consequence of defects in the FN-rich basement membrane surrounding the tube or could be a secondary effect of the absence of normal vascularization of the embryos.

If one postulates that the defects in the *FN.null* embryos arise from a deficit in mesoderm, the next question concerns the nature of the deficit; quantitative or qualitative? The mesoderm that does arise is obviously at least partially competent to carry out several characteristic mesodermal functions including induction of neural folds, formation of a primitive heart and formation of red blood cells (Figs 5, 6, 8). However, it is unclear whether various subclasses of mesodermal cells (notochord, presomite, endothelial) are present at normal levels and positions. This can be addressed using cell-type-specific markers. It is possible that cells determined for one or more of these fates are present in the *FN.null* embyros but fail to complete their morphogenesis and differentiation because they fail to reach their correct location or because they fail to organize their prospective structures. The latter interpretation would be consistent with localization of FN surrounding the notochord and somites, and in the vessel wall of the embryonic dorsal aorta (Fig. 7). In addition, disruption of β1 integrin adhesion changes somite cell shape in quail embryos (Drake et al., 1991). Future analyses should allow determination of which subsets of mesodermal cells are formed, reach their appropriate positions and are adhesive.

For the present, the results suggest that there is a definite, quantitative deficit in mesoderm formation. This could be a consequence of deficient adhesion, migration and/or proliferation. Comparison of normal and mutant littermates may reveal differences in embryonic cell proliferation in the absence of FN. Given the known effects of FN on cell migrations, a likely cause of the deficit in mesoderm is a deficit in cell migration. In normal embryos, the mesoderm emigrates from the primitive streak area in the posterior part of the embyro. From there the mesoderm moves laterally and axially between the ectoderm and endoderm as well as into the extraembryonic tissues (Nakatsuji et al., 1986; Tam and Beddington, 1987; Beddington, 1992; Lawson et al., 1991). A plausible model for the apparent shortage of mesoderm, both embryonic and extraembryonic, is that these movements or proliferation of these mesodermal cells are partially inhibited by the absence of FN in the *FN.null* embryos. Our present data do not allow us to distinguish between defects in migration and/or proliferation but future work with these mutant embryos should provide further insights into these questions.

One notable feature of the mutant embryos is the variability in phenotype observed. While some of this apparent variability could be due to asynchrony of development, it appears as if there are genuine differences in severity of the *FN.null* mutant phenotype. One possible explanation could arise from the mixed genetic background of the mice (129/Sv×C57BL/6). For example, strain differences in expression of another matrix molecule, which could partially substitute for FN, could produce such an effect. We are currently breeding the mutation onto pure genetic backgrounds to test this possibility. One of the most variable aspects is the presence or absence of a primitive heart (Figs 6, 8). If mesodermal movement is to some extent variable, then those structures furthest from the primitive streak (axial trunk positions, eg. somites) would always be most deficient, those that receive mesoderm by the shortest routes (allantois, head mesenchyme) would always be least affected and those in between, such as the heart, might be expected to be the most variable. Whether or not that explanation is valid, it is clear that primitive hearts, including beating muscle cells, can form in the absence of FN. This does not provide support for the model proposed by Linask and Lash (1986, 1988a,b), which proposed a requirement for precardiac cell migration on a FN gradient in chicken embryos. However, the embryonic mouse heart develops earlier and closer to the midline (Kaufman and Navaratnam, 1981). Those hearts that do form are not fully normal and lack a distinct endocardium (Fig. 8) consistent with the presence of FN in the endocardium of normal embryos (Fig. 7A) and in conformity with the generally poor development of endothelial structures in the *FN.null* mice.

Two other cell types, for which FN is proposed as a migratory substratum, are neural crest and primordial germ cells (see Introduction). We have not determined whether these cells appear and migrate in the mutant embryos; that will require suitable cell-type-specific markers. However, the mutant embryos do develop far enough that the early phases of these migrations may be accessible to study.

Finally, it is worth noting that the heterozygous *FN.null* mice also offer opportunities for study. These mice express half as much plasma FN as their normal littermates, indicating that the wild-type allele does not upregulate to compensate for the null allele. This may allow analysis of the enigmatic functions of plasma FN, which, though present at 0.5 μM, has no clearly understood function (Hynes, 1990). Many other potential functions will be testable in these mice, including wound healing, clearance of vascular debris and tumor suppression. To date, these mice have not shown a higher incidence of spontaneous tumors (unpublished data) but it should be informative to subject them to various forms of tumorigenesis. Thus, these lines of mice with a null mutation in the FN gene have already provided insights into the roles of FN during embryogenesis, confirming some preconceptions but refuting others. Further analyses should provide more information about other FN functions in development and in the physiology and pathology of adult mice.

We gratefully acknowledge Reinhard Faessler for helpful advice on the culture of ES cells, Doug Gray and Rudolf Jaenisch for the genomic library, Michael Rudnicki for PGK-neo, Janet Rossant for her subclone of D3-ES cells, Rolf Kemler for transgenic mice harboring a *neo* gene and Syntex Corporation for the gift of gancyclovir. We are particularly grateful to Ginny Papaioannou for helpful advice on interpreting the embryonic defects. We thank Steve Cornwall for technical assistance, Marge Cummisky for animal husbandry. We also thank Pam Norton, John Peters, Jane Trevithick, Lisa Urry and Gene Yee for helpful discussions regarding this project. E. L. G. was supported by the HHMI and by a Special Fellow grant from the Leukemia Society of America. E. N. G-L. was supported by the Centre Nationale de\ la Recherche Scientifique, NATO and by the Fondation Philippe and R. O. H. is an HHMI Investigator. This work was supported by the Howard Hughes Medical Institute and by a Program of Excellence grant from the National Heart, Lung and Blood Institute (HL41484).

REFERENCES

Armant, D. R., Kaplan, H. A. and Lennarz, W. J. (1986). Fibronectin and laminin promote in vitro attachment and outgrowth of mouse blastocysts. *Dev. Biol*. **116**, 519-523.

Beddington, R. S. P. (1992). Three dimensional representation of gastrulation in the mouse. *CIBA Foundation Symp.* **165**, 55-58.

Boucaut, J. C., Darribere, T., Boulekbache, H. and Thiery, J. P. (1984) Prevention of gastrulation but not neurulation by antibodies to fibronectin in amphibian embryos. *Nature* **307**, 364-367.

Bradley, A. (1987). Production and analysis of chimaeric mice. In *Teratocarcinomas and Embryonic Stem Cells: A Practical Approach*, (ed. E. J. Robertson), pp. 113-151. Oxford: IRL Press.

Brook, F. A., Shum, A. S. W., Van Straaten, H. W. M. and Copp, A. F. (1991). Curvature of the caudal region is responsible for failure of neural tube closure in the curly tail (*ct*) mouse embryo. *Development* **113**, 671-678.

Capecchi, M. R. (1989). Altering the genome by homologous recombination. *Science* **244**, 1288-1292.

Church, G. M. and Gilbert, W. (1984). Genomic sequencing. *Proc. Natl. Acad. Sci. USA* **81**, 1991-1995.

Clark, R. A. (1988). Potential roles of fibronectin in cutaneous wound repair. *Arch. Dermatol.* **124**, 201-206.

Copp, A. J., Brook, F. A. and Roberts, H. J. (1988). A cell-type-specific abnormality of cell proliferation in mytant (curly tail) mouse embryos developing spinal neural tube defects. *Development* **104**, 285-295.

Darribere, T., Boucher, D., Lacroix, J. C. and Boucaut, J. C. (1984). Fibronectin synthesis during oogenesis and early development of the amphibian *Urodeles waltlii*. *Cell Differ.* **14**, 171-177.

Darribere, T., Yamada, K. M., Johnson, K. E. and Boucaut, J. C. (1988). The l40-kDa fibronectin receptor complex is quired for mesodermal cell adhesion during gastrulation in the amphibian Pleurodeles waltlii. *Dev. Biol.* **126**, 182-194.

Doetschman, T. C., Eistetter, H., Katz, M., Schmidt, W. and Kemler, R. (1985). The *in vitro* development of blastocyst-derived embryonic stem cell lines: formation of visceral yolk sac, blood islands and myocardium. *J. Embryol. Exp. Morph.* **87**, 27-45.

Drake, C. J., Davis, L. A., Hungerford, J. E. and Little, C. D. (1991). Perturbation of β_1 integrin-mediated adhesions results in altered somite cell shape and behavior. *Dev. Biol.* **149**, 327-338.

Duband, J. L., Dufour, S., Yamada, S. S., Yamada, K. M. and Thiery, J. P. (1991). Neural crest cell locomotion induced by antibodies to β_1 integrins. A tool for studying the roles of substratum molecular avidity and density in migration. *J. Cell Sci.* **98**, 517-532.

Feinberg, A. P. and Vogelstein, B. (1983). A technique for radiolabeling DNA restriction endonuclease fragments to high specific activity. *Anal. Biochem.* **132,** 6-13.

ffrench-Constant, C. and Hynes, R. O. (1988). Patterns of fibronectin gene expression and splicing during cell migration in chicken embryos. *Development* **104**, 369-382.

ffrench-Constant, C., Hollingsworth, A., Heasman, J. and Wylie, C. C. (1991). Response to fibronectin of mouse primordial germ cells before, during and after migration. *Development* **113**, 1365-1373.

ffrench-Constant, C., Van De Water, Dvorak, H. F. and Hynes, R. O. (1989). Reappearance of an embryonic pattern of fibronectin splicing during wound healing in the adult rat. *J. Cell Biol.* **109**, 903-914.

Grabel, L. B. and Watts, T. D. (1987). The role of extracellular matrix in the migration and differentiation of parietal endoderm from teratocarcinoma embryoid bodies. *J. Cell Biol.* **105**, 441-448.

Harrisson, F. Van Nassauw, L., Van Hoof, J. and Foidart, J. -M. (1993). Microinjection of anti-fibronectin antibodies in the chicken blastoderm: inhibition of mesoblast cell migration but not of cell ingression at the primitive streak. *Anat. Rec.* (in press).

Heasman, J., Hynes, R. O., Swan, A. P., Thomas, V. and Wylie, C. C. (1981). Primordial germ cells of *Xenopus* embryos: the role of fibronectin in their adhesion during migration. *Cell* **27**, 437-447.

Hogan, B., Costantini, F. and Lacy, E. (1986). In *Manipulating the Mouse Embryo.* p. 175,176. Cold Spring Harbor, New York: Cold Spring Harbor Laboratory.

Hynes, R. O. (1990). *Fibronectins.* New York: Springer-Verlag.

Icardo, J. M., Nakamura, A., Fernandez-Teran, M. A. and Manasek, F. J. (1992). Effects of injecting fibronectin and antifibronectin antibodies on cushion mesenchyme formation in the chick. An *in vitro* study. *Anat. Embryol.* **185**, 239-247.

Johnson, K. E., Boucaut, J. C. and DeSimone, D. W. (1992). The role of the extracellular matrix in amphibian gastrulation. *Curr. Top. Dev. Biol.* **27**, 91-127.

Kaufman, M. H. (1992). *The Atlas of Mouse Development.* pp. 26-58. San Diego, California: Academic Press, Inc.

Kaufman, M. H. and Navaratnam, V. (1981). Early differentiation of the heart in mouse embryos. *J. Anat.* **133**, 235

Laemmli, U. K. (1970). Cleavage of structural proteins during the assembly of the head of bacteriophage T4. *Nature* **277**, 680-685.

Laird, P. W., Zijderveld, A., Linders, K., Rudnicki, M. A., Jaenisch, R. and Berns, A. (1991). Simplified mammalian DNA isolation procedure. *Nucl. Acids Res.* **19**, 4293.

Lallier, T. and Bronner-Fraser, M. (1990). The role of the extracellular matrix in neural crest cell migration. *Sem. in Dev. Biol.* **1**, 35-44.

Lawson, K. A., Meneses, J. J. and Pedersen, R. A. (1991). Clonal analysis of epiblast fate during germ layer formation in the mouse embryo. *Development* **113**, 891-911.

Lee, G., Hynes, R. and Kirschner, M. (1984). Temporal and spatial regulation of fibronectin in early Xenopus development. *Cell* **36**, 729-740.

Linask, K. K. and Lash, J. W. (1986). Precardiac cell migration:

fibronectin localization at mesoderm-endoderm interface during directional movement. *Dev. Biol*. **114**, 87-101.

Linask, K. K. and Lash, J. W. (1988a). A role for fibronectin in the migration of avian precardiac cells. I. Dose-dependent effects of fibronectin antibody. *Dev. Biol.* **129**, 315-323.

Linask, K. K. and Lash, J. W. (1988b). A role for fibronectin in the migration of avian precardiac cells. II. Rotation of the heart-forming region during different stages and its effects. *Dev. Biol.* **129**, 324-329.

Mansour, S. L., Thomas, K. R. and Capecchi, M. R. (1988). Disruption of the proto-oncogene *int-2* in mouse embryo-derive stem cells: a general strategy for targeting mutations to non-selectable genes. *Nature* **336**, 348-352.

Martins-Green, M. (1988). Origin of the dorsal surface of the neural tube by progressive delamination of epidermal ectoderm and neuroepithelium: implications for neurulation and neural tube defects. *Development* **103**, 687-706.

McBurney, M. W., Sutherland, L. C., Adra, C. N., Leclair, B., Rudnicki, M. A. and Jardine, K. (1991). The mouse Pgk-1 gene promotor contains an upstream activator sequence. *Nucl. Acids Res.* **20**, 5755-5761.

Mjaatvedt, C. H., Lepera, R. C. and Markwald, R. R. (1987). Myocardial specificity for initiating endothelial-mesenchymal transition in embryonic chick heart correlates with a particulate distribution of fibronectin. *Dev. Biol.* **119**, 59-67.

Nakatsuji, N., Snow, M. H. L and Wylie, C. C. (1986). Cinemicrographic study of the cell movement in the primitive-streak-stage mouse embryo. *J. Embryol. Exp. Morph.* **96**, 99-109.

Ostrovsky, D., Cheney, C. M., Seitz, A. W. and Lash, J. W. (1983). Fibronectin distribution during somitogenesis in the chick embryo. *Cell Differ*. **13**, 217-223.

Patel, V. P. and Lodish, H. F. (1987). A fibronectin matrix is required for differentiation of murine erythroleukemia cells into reticulocytes. *J. Cell Biol.* **105**, 3105-3118.

Rider, V. Carlone, D. L., Witrock, D., Cai, C. and Oliver, N. (1992). Uterine fibronectin mRNA content and localization are modulated during implantation. *Dev. Dynam.* **195**, 1-14.

Risau, W. (1991). Vasculogenesis, angiogenesis and endothelial cell differentiation during embryonic development. In *The Development of the Vascular System* (ed. R. N. Feinberg, G. K. Sherer and R. Auerbach), **14**, 58-68.

Risau, W. and Lemmon, V. (1988). Changes in the vascular extracellular matrix during embryonic vasculogenesis and angiogenesis. *Dev. Biol.* **125**, 441-450.

Rudnicki, M. A., Braun, T., Hinuma, S. and Jaenisch, R. (1992). Inactivation of MyoD in mice leads to up-regulation of the myogenic HLH gene Myf-5 and results in apparently normal muscle development. *Cell* **71**, 383-390.

Sutherland, A. E., Calarco, P. G. and Damsky, C. H. (1988). Expression and function of cell surface extracellular matrix receptors in mouse blastocyst attachment and outgrowth. *J. Cell Biol.* **106**, 1331-1348.

Tam, P. P. L. and Beddington, R. S. P. (1987). The formation of mesodermal tissues in the mouse embryo during gastrulation and early organogenesis. *Development* **99**, 109-126.

Thiery, J. P., Duband, J. L. and Tucker, G. C. (1985). Cell Migration in the vertebrate embryo: Role of cell adhesion and tissue environment in pattern formation. *Annu. Rev. Cell Biol.* **1**, 91-113.

Thorsteinsdottir, S. (1992). Basement membrane and fibronectin matrix are distinct entities in the developing mouse blastocyst. *Anat. Rec.* **232**, 141-149.

Wartiovaara, J., Leivo, I. and Vaheri, A. (1979). Expression of the cell surface-associated glycoprotein, fibronectin, in the early mouse embryo. *Dev. Biol.* **69**, 247-257.

Wedlich, D., Hacke, H. and Klein, G. (1989). The distribution of fibronectin and laminin in the somitogenesis of *Xenopus laevis*. *Differentiation* **40**, 77-83.

Zetter, B. R. and Martin, G. R. (1978). Expression of a high molecular weight cell surface glycoprotein (LETS protein) by preimplantation mouse embryos and teratocarcinoma stem cells. *Proc. Natl. Acad. Sci. USA* **75**, 2324-2328.

(Accepted 7 September1993)